

Time Resolved PIV Measurements of the Flow Field Associated With the Interaction of Concentrated and Distributed Vorticity

H. U. Ain¹, J. R. Elsna¹ and J. C. Klewicki^{1,2}

¹Department of Mechanical Engineering
University of Melbourne, Parkville, VIC 3010, Australia

²Department of Mechanical Engineering
University of New Hampshire, Durham, New Hampshire 03824, USA

Abstract

Time resolved particle image velocimetry was used to investigate new aspects of the flow field associated with a vortex ring/moving wall interaction. These physical simulations represent aspects of the instantaneous flow field interactions known to exist in turbulent wall-bounded flows. To allow for an explicit study of these interactions and avoid background turbulence, unsteady, laminar, vortex ring experiments were conducted with reproducible initial conditions. For the case when the vorticity in the bottom core of the ring and shear layer have opposite sign, the passage of the vortex ring above the wall results in a lifting of the near wall fluid. This gives rise to the formation of a primary hairpin vortex with the same sign vorticity as the top core of the vortex ring. The results obtained indicate that the ring rebounds from the wall for these interactions at increasing angles for increasing incident angles. Furthermore, the hairpin lift up occurs over shorter time scales when the incidence angle of the vortex ring was increased. The results provide further insight into how vortical structures interact and the associated momentum transport mechanisms relevant to turbulent flows.

Introduction

Vortical motions play a vital role in turbulence production, dissipation and time-averaged turbulence statistics. Therefore, it is important to understand what flow features are responsible for the inertial mechanisms of turbulence, and ultimately the mean distribution of momentum. A variety of past experimental and numerical studies suggest the presence of distinctive coherent regions within the vorticity field of wall-bounded turbulent flows, commonly termed “hairpin vortices” [1]. These coherent structures, thought to be a basic building block of wall-turbulence, have been used in models for the turbulent boundary layer [11].

Chu & Falco [5] used flow visualization to mimic features observed in the turbulent boundary layer by convecting a vortex ring (Falco’s *typical eddies*) towards or away from a moving wall. They proposed that the relevant interactions within the turbulent boundary layers can be probabilistically grouped into four categories based upon stability considerations (see [5] for nomenclature). Dupont et al. [6] used an experimental set up similar to [5], but used advanced measurement techniques, particle image velocimetry (PIV) and particle tracking velocimetry (PTV) for detailed characterization of what Chu & Falco called a type II interaction. A type II interaction features a hairpin vortex formation and vortex ring rebound, with the ring remaining coherent throughout. Their findings indicate that the vortex ring acted as an external perturbation that resulted in Stokes layer lift up, thereby producing a hairpin. These authors pointed out that the study of Type III and Type IV interactions, where the ring becomes unstable, would be interesting to study as they lead to turbulence, but are difficult to characterize due to their unstable nature.

The studies by Haidari and Smith [8] examined vortex dynamics near a wall in a well-controlled environment. Their results provide important clarity regarding asymmetries inherent in the generation and regeneration of hairpin like vortices, and their contribution towards turbulent inertia. Their experimental studies described that the lasting contribution to the mean Reynolds stress (turbulent inertia) are made during events causing surface layer eruptions followed by the roll up of sheets of vorticity, and these events continue to occur repeatedly. Another important conclusion drawn from their analysis is that in high shear flows, a small amount of local asymmetry can give rise to much larger asymmetry for a single vortex or combination of vortices. This motivates the fact that those interactions that leave a signature on the mean dynamics must contain asymmetries associated with their geometry or kinematics. The numerical examination of vorticity field in a transitional boundary layer by Bernard [3] suggests that shearing of spanwise vorticity beyond the viscous sublayer creates a wall normal vorticity away from the boundary, which subsequently causes the appearance of streamwise vorticity shaping into a hairpin structure.

In this paper, we report on experiments investigating velocity-vorticity interactions that underlie the dynamical mechanisms by which turbulent motions redistribute momentum. The aim is to understand the influence of the incidence angle, α , of the vortex ring on a Type II interaction and the transition into Type III. It is an extension of the study by Chu & Falco [5] since their observations were qualitative. The scope of this study is to present the new observations on the vortex ring/moving wall simulation and to characterize vortex ring properties. It is thought that by understanding the details of the interaction, further insight can be gained into the generic mechanisms operative in wall-bounded and other turbulent flows.

Experimental Facility

The vortex ring apparatus (VRA) consists of a piston-cylinder connected to a seamless, stainless steel vortex generator tube using a flexible 38.1 mm tubing. The ring generator tube is 80 cm long, with an internal diameter of 3.48 cm. The piston motion is precisely controlled using LabView software and a stepper motor. A vortex ring is generated at the exit of the tube by converting rotational motion from the stepper motor into translation, using a threaded rod. Vortex rings are formed using a stroke length, L/D of 2.0, where L is the fluid displacement and D is the tube diameter. The Reynolds number of the ring is 2960 (based upon an average slug velocity, $\overline{V}_s = 1/T \int v_s(t) dt$ and tube diameter). The piston velocity is kept fixed for the results reported herein. A time developing shear layer, i.e., a Stokes layer, is generated using a conveyor belt that is 305 mm wide and 1.83 m long. The belt rides on a nominally flat acrylic plate and is driven by a servo motor and a timing belt system. To start the belt impulsively, trapezoidal velocity profiles are implemented in LabView where the acceleration time is much

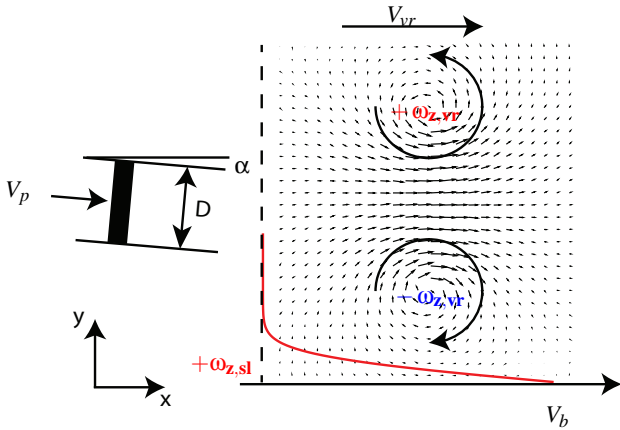


Figure 1: Schematic representation of a vortex ring and shear layer interaction.

less than the overall time interval, T . A laminar Stokes layer develops with time. The belt continually operates until the vortex ring passes through the field of view. The thickness of the Stokes layer scales with \sqrt{t} . Thus, the thickness of Stokes layer is essentially constant as the ring advects through the field of view, since the total image acquisition time is less than 8 seconds. The belt propagates in the same direction as the vortex ring, providing the opportunity to explore opposite sign vorticity interactions between the bottom lobe of the vortex ring and shear layer. The belt velocity, V_b , used for the present study is 7.9 cm/sec. The VRA apparatus and the conveyor belt are installed in a large water tank with dimensions 3.6m (L) x 1.08m (W) x 0.37m (H). The glass tank is filled with water maintaining a constant water level to ensure constant hydrostatic pressure for repeatability and consistent boundary conditions in each experiment.

Data Acquisition Technique

Time resolved PIV is used to acquire image pairs at a rate of 15 Hz, using two sCMOS cameras with resolution 2560 x 2160 *pixel*, placed side by side to obtain a large field of view (FOV). The streamwise overlap between the cameras FOV is 1 cm. The FOV starts 2/3D from the termination point of the vortex generation tube and the size of the FOV is 7.1D x 3.1D. Illumination of particles is achieved using a double-pulsed 532nm Nd:YAG laser rated at 200mJ/pulse. Pulse generators synchronize the sCMOS cameras and laser Q-switch timing. Entire water tank is seeded with neutrally buoyant, 10 μm hollow glass sphere particles from Dantec Dynamics. The time delay, Δt , between image capture is 4 ms. The maximum particle displacement is 8 to 10 pixels. The centreline of the vortex generator tube is 1.5D from the conveyor belt in the wall-normal direction for all the cases presented herein.

Data Reduction

The acquired images are processed using an in-house PIV package that utilizes a standard multi-pass, multigrid, cross-correlation algorithm [4]. A base interrogation window size of 32 x 32 *pixel* is utilized in the first pass, followed by a 16 x 16 *pixel* window size with 50% overlap for the second pass. The spatial resolution of velocity vectors in both the streamwise and wall-normal directions is 0.01D. To correct for the random Gaussian modulation of vortex trajectory [9], the instantaneous velocity vectors are phase and conditionally averaged on the location of the maximum spanwise vorticity and

$Re_{vr} = 2960, \zeta_{sl}/\zeta_{vr} = 0.65$		
Case	α°	δ^*/D
1, \diamond	0	-
2, \triangleleft	3	0.67
3, \square	12	0.1

Table 1: Experimental parameters and symbols for the cases presented herein. The formation circulation for the ring is $\bar{V}_s 2D$ and for the shear layer, $V_b D_c$, where D_c is the distance between vortex cores.

the ring centerline angle with respect to the wall. The spatial averaging is employed for 100 instantaneous realizations in each case. The spanwise vorticity, ω_z , is obtained by differentiating the velocity field using a 4th order Richardson extrapolation scheme [7]. The circulation, ζ , on the upper and lower half of the ring is obtained by Stokes' theorem, $\int_A \omega_z dA$, using an elliptical integration domain around the ring. The uncertainty in circulation and vorticity measurement is $\pm 0.24\%$ and $\pm 0.45\%$ respectively.

Results and Discussion

Experimental parameters and the symbol definitions are presented in table 1. The Stokes layer experimental velocity profile is in good agreement with the analytical solution [2]. The vortex ring at 0° , case 1 (base case), is not time resolved, but is used for comparison purposes. The base case refers to unperturbed vortex rings over a stationary wall.

When perturbed by the vortex ring, the Stokes layer, a vortex sheet of finite thickness, reorganizes into a lifting hairpin vortex. The various types of evolution are governed by different initial and geometric conditions. A time sequence of the spanwise vorticity contours for case 2 is shown in figure 2. Since the vortex ring and hairpin do not intermix, this is a type II/stable interaction in which both the vortex ring and hairpin vortex remain distinct and coherent. The vorticity is scaled with the maximum vorticity at each location in the ring. Early x^* contours show evidence of a hairpin vortex in the perturbed state which in developed state is oriented at about 45° [2]. The legs of the hairpin vortex cannot be observed in this study as data are obtained on the center-plane of the ring.

Previous studies have identified the angle of incidence, the velocity ratio between the ring and the wall and the boundary layer thickness as the critical parameters that govern the stability of the interaction between an impinging vortex ring and a moving wall. Stable interactions occur at shallow angle of incidence and well developed boundary layer [5]. Liang [10] indicated that for angles greater than 9° , the interactions are unstable for a ring to wall velocity ratio of 0.8, irrespective of boundary layer thickness. The ring to wall velocity ratio for the present study is 1.1, and ratios less than 0.8 cannot be investigated due to mechanical system limitations. To examine a so-called type III (unstable) interaction, the ring is convected towards the wall at 12° when the dimensionless displacement thickness is 0.1 (case 3). The time progression of this case is presented in figure 3. The hairpin vortex lifts up quickly as shown in the early x^* contours. At $t^+ = 27$, the hairpin vortex appears to be attracted towards the center of the vortex ring. A kink appears just above the hairpin vortex head and at $t^+ = 28$ this portion becomes distinct, suggesting that the lifted hairpin vortex pinches off. At this instant, the bottom lobe of the vortex ring is 0.8 cm above the wall. The ring still appears intact and changes its direction of flight. At later times, the ring diffuses, but still maintains its structure as a ring. The hairpin vortex disintegrates completely with no inges-

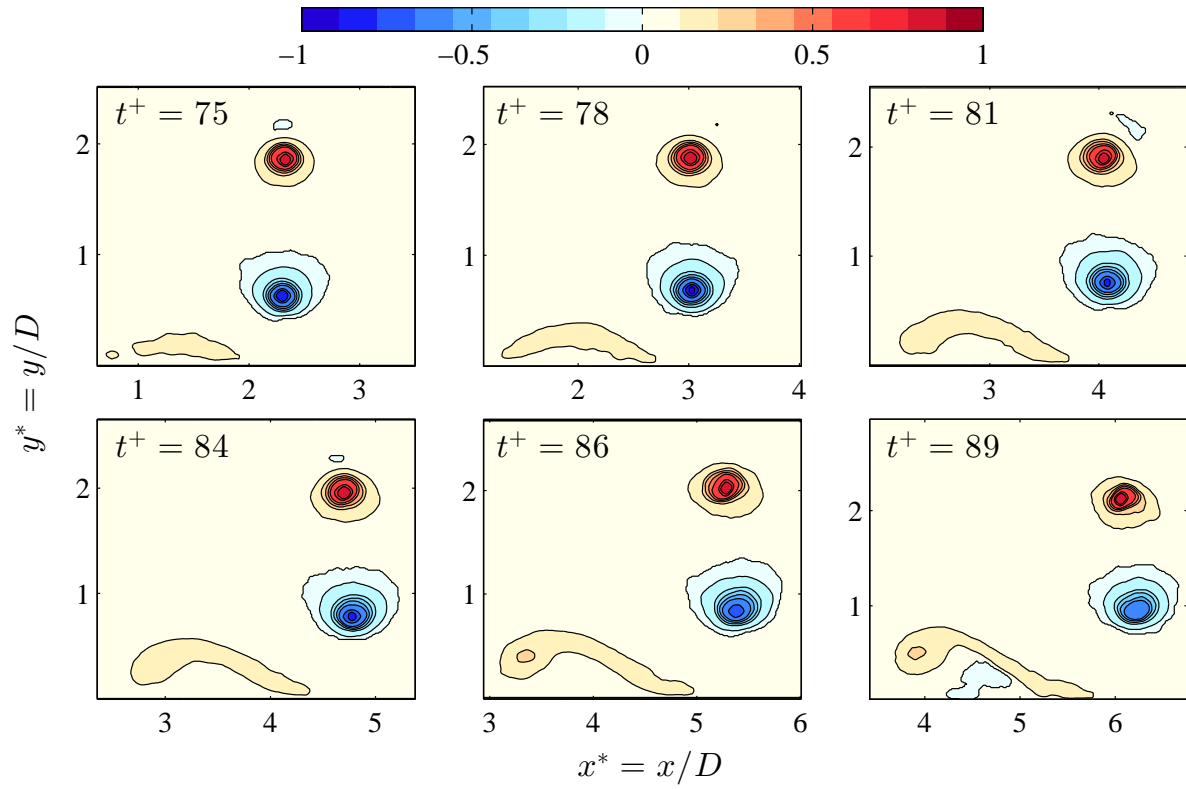


Figure 2: Contours of the conditionally averaged spanwise vorticity for case 2 normalized with $\omega_{z,vr,max}$. The vortex ring is travelling from left to right. Time is dimensionless using the belt velocity and tube diameter, $t^+ = tV_b/D$.

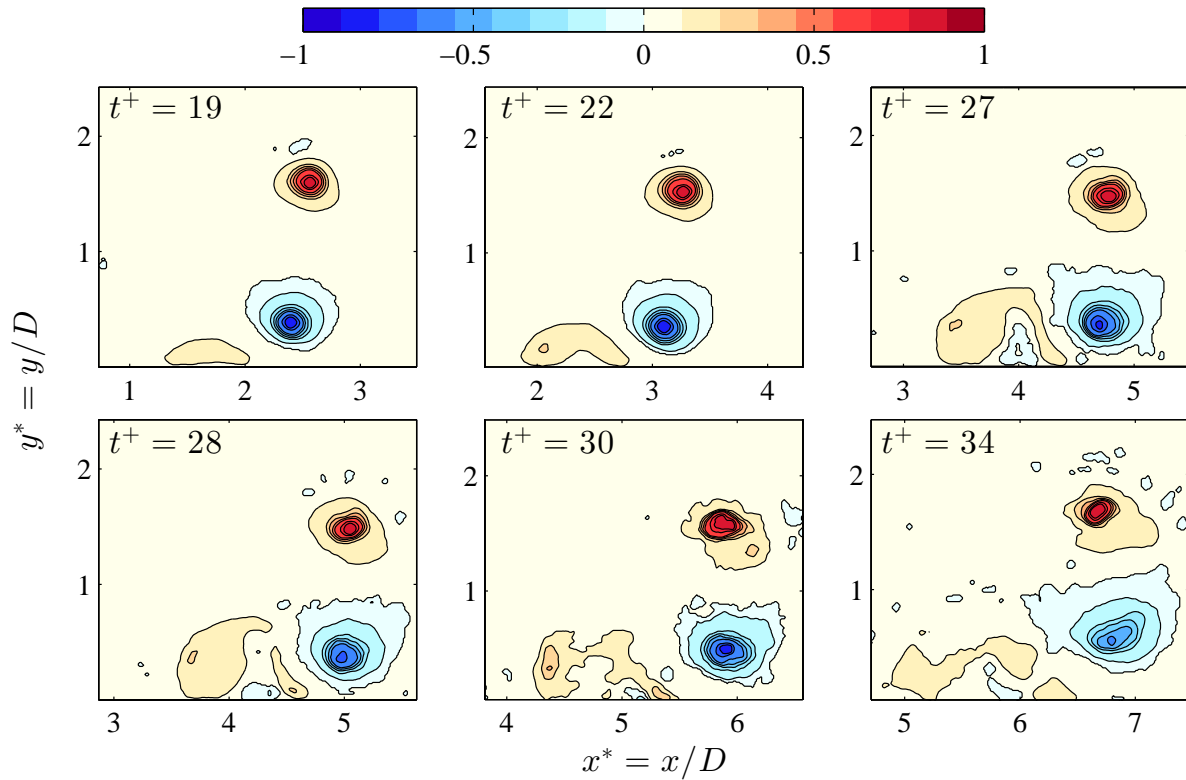


Figure 3: Contours of the conditionally averaged spanwise vorticity for case 3. See figure 2 caption for details.

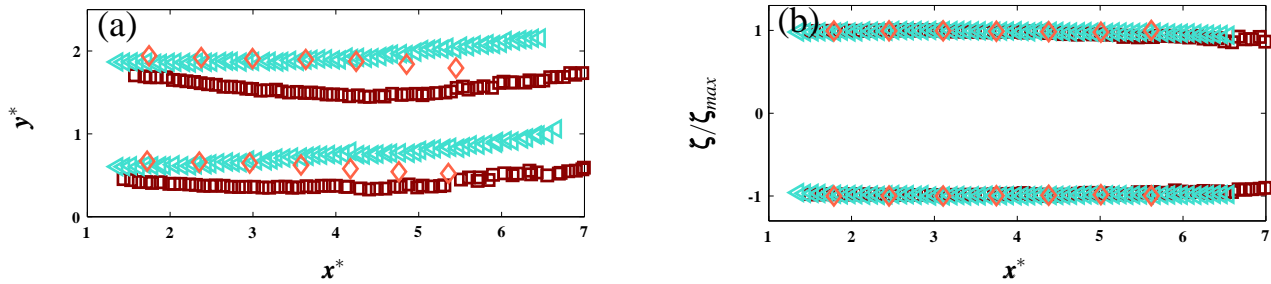


Figure 4: (a) Trajectory of the minimum and maximum spanwise vorticity, ω_z , for the vortex ring, (b) Circulation ratio of the vortex ring normalized by the maximum $\zeta_{vr,max}$.

tion into the ring. This observation is inconsistent with previous studies where an unstable interaction resulted in hairpin ingestion into the ring followed by the breakup of both the ring and hairpin vortices.

In general, the hairpin lift up coincides with the ring changing trajectory. To illustrate the influence of the angle of incidence on the ring direction of motion, the trajectory of the vortex cores are presented in figure 4 (a). These are obtained at the locations of maximum and minimum spanwise vorticity in the ring. The trajectory of the base case indicates that the ring starts to move slightly towards the wall which is attributed to a subtle wall effect. The 3° trajectory bends away from the wall after the hairpin vortex lift up. This is clearly evident around $x^* = 3.5$. The trajectory for 12° indicates that the ring comes closer to the wall as compared to the 3° case. The ring changes its direction of motion at $x^* = 4.5$ and moves away from the wall. The apparent lift force leading to this is potentially attributed to an increased interaction between the bottom lobe of the ring and shear layer altering the bottom lobe circulation, and nearly constant top lobe circulation. The circulations in the top and bottom lobes of the ring are presented in figure 4 (b). The bottom lobe circulation for 12° experiences a 2.5% change from its initial value and occurs at the location where the minimum in trajectory is observed. The top lobe circulation remains unaffected. The changes in overall balance of top lobe circulation are not noticeable until $x^* = 5.5$. From the point of rebound after until last x^* location, the top and bottom lobe circulation decays by 10% due to viscosity. The overall change in circulation for the 3° case remains within 3% from initial to final x^* locations. At shallow angles, the ring does not get close enough to the wall, explaining the shallow rebound. The wall layer thickness dictates the degree of interaction between the ring and shear layer at large angles since the amount of vorticity in the layer, i.e., its circulation, is equivalent. The slight alterations in ring circulation when the ring rebounds is indicative of the fact that there may be other factors, e.g. induced velocity, contributing towards the dynamics of the interaction.

Conclusions

An experimental investigation on the interaction between angled vortex rings and a moving wall is reported. The results indicate that the compact regions of vorticity are stable, strongly coherent and relatively long lived features of the flow which may contribute significantly to the momentum transport. Furthermore, the results present new aspects of vortex ring/moving wall interactions, which do not fully support the turbulence production model proposed by previous studies. It is thought that Type II interaction is the most representative of the hairpin generation process and Type III interaction is not evident in the present study.

Acknowledgements

The authors gratefully acknowledge financial support provided by the Australian Research Council, grant number DP110102896.

References

- [1] Adrian, R.J., Hairpin vortex organization in wall turbulence, *Phys. Fluids*, **19**, 2007.
- [2] Ain, H.U. and Elsnab, J.R. and Klewicki, J.C., Experimental investigation of momentum transport associated with the interaction of concentrated and distributed vorticity, in *Proceedings of the 19th Australasian Fluid Mechanics Conference*, editors H. Chowdhury, F. Alam, Melbourne VIC Australia : RMIT University, 2014, 247.
- [3] Bernard, P.S., Boundary Layer Vorticity and the Rise of Hairpins, in *Lille Workshop: Progress in wall turbulence: understanding and modelling*, editors M. Stanislas, J. Jimenez, I. Marusic, Springer, 2014, 159–169.
- [4] Chauhan, K., Philip, J., de Silva, C. M., Hutchins, N. and Marusic, I., The turbulent/non-turbulent interface and entrainment in a boundary layer, *J. Fluid Mech.*, **42**, 2014, 119–151.
- [5] Chu, C.C. and Falco, R.E., Vortex ring/viscous wall layer interaction model of the turbulence production process near walls, *Exp. Fluids*, **6**, 1988, 305–315.
- [6] Dupont, P., Croisier, G., Werquin, O. and Stanislas, M., DPIV, HPTV and visualization study of a vortex ring-moving wall interaction, *Exp. Fluids*, **33**, 2002, 555–564.
- [7] Foucaut, J. M. and Stanislas, M., Some considerations on the accuracy and frequency response of some derivative filters applied to particle image velocimetry vector fields, *Meas. Sci. Technol.*, **13**, 2002, 1058–1071.
- [8] Haidari, A.H. and Smith, C.R., The generation and regeneration of single hairpin vortices, *J. Fluid Mech.*, **277**, 1994, 135–162.
- [9] Jammy, S.P., Hills, N. and Birch, D.M., Boundary conditions and vortex wandering, *J. Fluid Mech.*, **747**, 2014, 350–368.
- [10] Liang, S., Experimental investigation of vortex ring/ moving wall interactions, *MS thesis, Dept. Mech. Eng. Michigan State Univ*, 1984.
- [11] Smith, C.R. and Walker, J.D.A. and Haidari, A.H. and So-brun, U., On the dynamics of near-wall turbulence, *Phil. Trans. R. Soc. Lond. A*, **336**, 1991, 131–175.